SELF-HEALING CAPABILITY OF STRAIN-HARDENING FIBER REINFORCED GEOPOLYMER COMPOSITES

Motohiro OHNO¹, Taeho KIM², Victor C. LI³

- 1. Assistant Professor, Department of Civil Engineering, the University of Tokyo, Tokyo, Japan
- 2. Graduate Student, Department of Mechanical and Civil Engineering, California Institute of Technology, Pasadena (CA), USA
- 3. Professor, Department of Civil and Environmental Engineering, University of Michigan, Ann Abor (MI), USA

Corresponding author email: ohno@concrete.t.u-tokyo.ac.jp

Abstract

This study reports on the self-healing capability of a strain-hardening fiber reinforced geopolymer composite, named Engineered Geopolymer Composite (EGC). EGC specimens were first uniaxially loaded to a tensile strain of 1%. The cracked specimens were then subjected to three different conditioning regimes: air curing, water curing, and no curing (i.e. reloading right after the preloading). Stiffness reduction was measured for each series by comparing the initial stiffness of intact specimens and the residual stiffness of the cracked specimens. In the water-cured specimens, white precipitates were observed in microcracks formed by preloading. Experimental results of the series showed significant stiffness recovery for low stress levels in the range of 0.5 – 1.0 MPa. Self-healing products observed by using a scanning electron microscope were mostly angular, stone-like substance. An analysis of energy dispersive spectroscopy showed that the healing products were relatively rich in silicon (Si) and aluminium (Al) and had lower concentration of calcium (Ca), compared to the geopolymer matrix phase. This implies that main product of EGC self-healing is unlikely to be either calcite (CaCO₃) or salt deposits such as Na₂CO₃, but rather a formation of some aluminosilicate compounds. This study provides a baseline for further investigations into the development of geopolymer composites with robust self-healing.

Keywords: Self-healing, Geopolymer, Strain-hardening, Fiber reinforced composite, Stiffness recovery

1. introduction

Self-healing concrete is attractive to many countries facing a huge financial burden for repair and rehabilitation of their aging infrastructure. Today, various types of self-healing concrete and relevant technologies have been developed, including encapsulation of healing chemicals (Huang and Ye 2011) or calcite-producing bacteria (Jonkers et al. 2010), inclusion of mineral admixture (Ahn and Kishi 2010), and healing agents activated by a heating device embedded in the cement matrix (Nishiwaki et al. 2006).

Engineered Cementitious Composite (ECC) is another promising technology for robust self-healing concrete. ECC is a family of strain-hardening fiber reinforced cementitious composites featuring high tensile ductility and multiple microcracking characteristics. Previous studies have experimentally demonstrated the self-healing functionality of ECC with significant mechanical performance recovery, repeatability, and versatility (Qian, Zhou and Schlangen 2010, Kan et al. 2010, Li and Li 2011, Herbert and Li 2013, Suryanto et al. 2015). The robust self-healing of ECC is mainly achieved through the self-controlled microcracking; the tight crack width enables intrinsic healing functionality of cement materials, allowing healing products to precipitate and fully seal the cracks.

Self-healing phenomena have been also reported for geopolymer, which is a family of alkaliactivated aluminosilicate binder materials (Duxson et al. 2007). Ahn and Kishi (2010) found that the addition of geo-materials, which were mainly composed of SiO₂ and sodium aluminium silicate hydroxide, to an ordinary Portland cement (OPC) binder leads to formation of a geopolymeric gel between cracks. It was suggested that alkali activation of the geo-materials produced an amorphous calcium product of fly ash-based geopolymer. On the other hand, Liu et al. (2017) and Ali et al. (2015) reported self-healing of fly ash-based geopolymer itself. Both studies suggested that formation of additional geopolymer gels from unreacted fly ash particles contributed to recovery in compressive and flexural strengths. It should be noted, however, that self-healing in geopolymer is a relatively new research area and the literature on the subject is still limited.

Recently, a family of strain-hardening fiber reinforced geopolymer composites – named Engineered Geopolymer Composite (EGC) – has been developed (Ohno and Li 2014). EGC has comparable tensile and flexural properties to ECC, including high tensile ductility and tightly-controlled multiple microcracking with crack width of less than 50 µm. This tight crack width would be favourable for maximizing the healing functionality of the geopolymer matrix, as in cement-based materials. In fact, the self-healing capability of a fiber reinforced geopolymer composite produced from fly ash and metakaolin has been reported by Kan et al. (2019).

This paper presents an experimental study on the self-healing capability of fly ash-based EGC. EGC specimens are first uniaxially loaded to a tensile strain of 1%. The cracked specimens are then subjected to three different conditioning regimes prior to reloading: air curing, water curing, and no curing (i.e. reloading right after preloading). Cracks are photographically recorded regularly to capture the formation of healing products during the conditioning. To evaluate the stiffness recovery due to self-healing, stiffness reduction is measured for each series by comparing the initial stiffness of intact specimens and the residual stiffness in reloading. In addition, the microstructure of healing products is observed by using a scanning electron microscope (SEM), and an elemental analysis is conducted by using an energy dispersive spectroscopy (EDS) analyser.

2. Materials and methods

2.1. Materials and mix design

Table 1 lists the mix design of EGC used in this study. Two types of fly ash were blended in the mixture (labelled "Fly ash A" and "Fly ash B"). Both are classified as class F fly ash as designated by ASTM C 618. Table 2 lists their chemical compositions reported by the manufacturer. The density and fineness (percent retained on 45 μm sieve) are 2.58 g/cm³ and 22.24% for Fly ash A, and 2.53 g/cm³ and 16.58% for Fly ash B. F-75 Ottawa silica sand was used as aggregate. The alkaline activator was prepared by dissolving laboratory-grade sodium hydroxide (NaOH) pellets in mixture of tap water and sodium silicate solution (Na₂SiO₃ with 8.9 wt% Na₂O, 28.7 wt% SiO₂, and 62.5 wt% H₂O). The solution was prepared at least 24 hours before its use as activator so that chemical equilibrium was attained. Additional water (labelled "Mix water") was used during mortar mixing to obtain desired rheology of the fresh mortar for achieving good fiber dispersion. Polyvinyl alcohol (PVA) fibers with 1.2% oil coating by weight were employed as in a standard ECC. The fiber volume fraction was 2% of the composite. Physical properties of the PVA fibers can be found elsewhere (Ohno and Li 2018).

Alkaline activator Fly ash A Fly ash B Sand Na₂SiO₃ NaOH Water Mix water PVA fiber 0.6 0.4 0.2 0.225 0.044 0.031 0.10 0.021

Table 1. EGC mix design (by mass).

Table 2. Chemical compositions of fly ash (mass %).

	SiO ₂	Al_2O_3	Fe_2O_3	CaO	SO_3	MgO	Na ₂ O	K ₂ O	Moisture	LOI
Fly ash A										1.99
Fly ash B	42.20	22.51	9.20	15.66	1.85	3.20	0.98	1.53	012	1.34

2.2. Specimen preparation

Fly ash and silica sand were first dry-mixed for 2 minutes. The activator solution and mix water were then added to the mixture. After the fresh mortar reached the desired rheological state, PVA fibers were

slowly added, and mixing was continued until the fibers were properly dispersed. The mixture was cast into molds on a vibration table, and then cured at room temperature $(23 \pm 3 \, ^{\circ}\text{C})$ for 24 hours. Subsequently, the hardened specimens were cured in an oven at 60 $^{\circ}\text{C}$ for another 24 hours, followed by air curing at room temperature prior to testing.

Twelve dogbone-shaped specimens were prepared for stiffness recovery measurement. The rectangular gauge section of specimens measured 80 mm in length, 30 mm in width, and 13 mm in thickness. Two additional dogbone specimens were also prepared, which incorporated no silica sand and were investigated by using SEM and EDS. The silica sand was excluded so that specimens consisted of only components involved in self-healing (i.e. geopolymer paste, fibers, and self-healing products).

2.3. Stiffness recovery measurement

Twelve Specimens for stiffness recovery measurement were divided into 4 groups of 3 specimens each, referred to as "W-1%", "A-1%", "N-1%", and "W-0%". Specimens in the first three groups were uniaxially loaded to a tensile strain of 1% at the age of 28 days, while those of W-0% series were not preloaded. The tensile testing was conducted under displacement control at the rate of 0.5 mm/min. Two linear variable displacement transducers (LVDTs) were attached on each specimen to measure extensions within the gauge length. Tensile strain was computed from the average of extensions divided by the gauge length.

Preloaded specimens of W-1% series were cured in water for 120 days. The specimens were then air-dried for at least 24 hours, followed by reloading in the identical test configuration. On the other hand, specimens of A-1% were cured in air for 120 days prior to reloading. Microcracks in both series were regularly photographed during the curing, using a digital optical microscope.

In the case of N-1% series, specimens were preloaded to 1%, unloaded, and then reloaded on the same day with no conditioning. This series was a control series to determine the stiffness reduction due to the applied 1% strain. The reduction in N-1% was compared with those of W-1% and A-1% to evaluate their stiffness recovery.

It should be mentioned that aside from the self-healing phenomenon, the 120-day water curing and corresponding aging of the specimens could alter the matrix and fiber/matrix interface properties, which might have some effect on the stiffness. Thus, W-0% specimens were used to evaluate this effect. The specimens were not preloaded but subjected to water curing from the age of 28 days for 120 days (i.e. the same conditioning as that for W-1% series). After air-dried for at least 24 hours, specimens were uniaxially loaded to measure the stiffness. The initial stiffness of W-1% at the age of 28 days was compared to the stiffness of the intact W-0% series that was measured after 120-day water curing.

For stiffness measurement, chord modulus was used in this study, as in a prior study on self-healing ECC (Herbert and Li 2013). Chord modulus is the slope of the line drawn between two specified points on the stress-strain curve and is calculated by using the following equation:

$$E_{\sigma_b - \sigma_a} = \frac{\sigma_b - \sigma_a}{\varepsilon_b - \varepsilon_a} \tag{1}$$

where σ_b and σ_a are stresses at two specified points (defined in Section 3.2), and ε_b and ε_a are the corresponding strains. Stiffness ratio (R) is defined as the ratio of residual stiffness at reloading (E') to initial stiffness at preloading (E):

$$R_{\sigma_b - \sigma_a} = \frac{E'_{\sigma_b - \sigma_a}}{E_{\sigma_b - \sigma_a}} \tag{2}$$

2.4. Self-healing product characterization

Two specimens incorporating no sand (named SEM-1% series) underwent the same preloading and conditioning as those for W-1%. After the 120-day water curing, a small prism that contained a microcrack and healing products within the crack was cut from a specimen. Dimensions of the prism were roughly 20 mm in length, 30 mm in width, and 13 mm in thickness. Grinding and polishing were not applied to prevent damage of the healing products.

For SEM observation, a large-field detector that captures secondary electrons was used in a low-vacuum environment. For the elemental analysis of healing products, an EDS analyzer equipped with

the SEM was used. The accelerating voltage and spot size were 10 kV and 0.23 nA, respectively. Samples for SEM and EDS were prepared without additional coating (gold, etc.)

Elemental compositions were analyzed along a line segment that crossed a microcrack and healing products, starting from the uncracked region of the composite as shown in Figure 1. Since the surface analyzed by EDS should be flat enough for accurate characterization, a region where healing products fully sealed a microcrack was selected for the line-scan analysis. The line segment was 78 μm long with the scanning interval of 0.08 μm. Detected elements were carbon (C), oxygen (O), iron (Fe), sodium (Na), magnesium (Mg), aluminum (Al), silicon (Si), phosphorous (P), sulfur (S), and potassium (K). The atomic percent of each element was calculated as x-ray counts for the element divided by the total counts for all elements. This line-scan function detected the relative difference in chemical compositions between the EGC matrix and healing products. In addition, a map scan was conducted to overlay element concentration on top of the SEM image, visualizing the relative difference over the entire region.

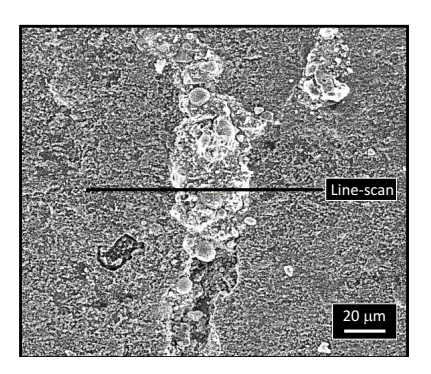


Figure 1. EDS line-scan analysis performed on a line crossing a microcrack sealed with white precipitates.

3. Results and discussion

3.1. Degree of healing product formation

During water curing, white precipitates were observed within microcracks of W-1% and SEM-1% specimens. The maximum residual crack width was less than 30 µm in all specimens. Despite the tightly controlled microcracks, the degree of precipitation was variable from crack to crack as shown in Figure 2; some cracks were completely sealed with the white residue, while some cracks were only partially sealed. It appeared that smaller crack widths generally resulted in higher degree and rate of healing product formation. According to Kan et al. (2010), crack width of less than 50 µm in ECC specimens leads to robust self-healing, and most cracks below this width are completely healed. Thus, self-healing in EGC investigated in this study was limited compared to that in ECC.

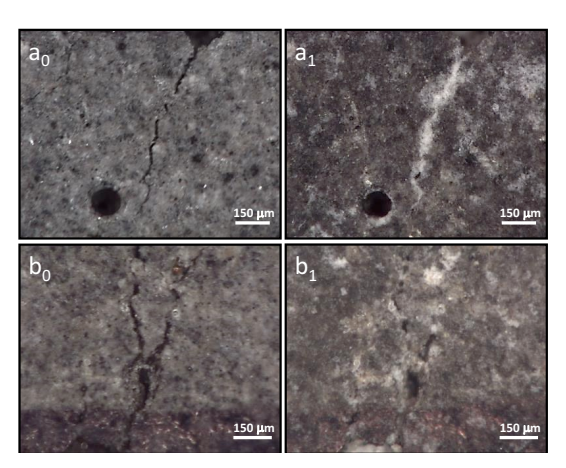


Figure 2. Images of two microcracks in W-1% (a₀, b₀) right after preloading and (a₁, b₁) after water curing.

In A–1% series, no white substance was observed during the 120-day air curing, although the number of cracks and crack width distribution were similar to those of W–1% series. Yang, Yang and Li (2011)

reported that air-cured ECC specimens also showed no significant healing. Therefore, it seems that the presence of water also plays an important role in self-healing of EGC investigated in this study.

However, the results and discussion above contradict a previous study by Kan et al. (2019); they studied self-healing of EGC prepared by fly ash and metakaolin, and found that air-cured specimens exhibited a higher healing functionality than specimens subjected to wet-dry cycles. From results of EDS, X-ray diffraction (XRD), and Fourier transform infrared spectroscopy (FT-IR), they concluded that healing products were mainly amorphous aluminosilicate resulted from geopolymerization. As water is not an active reactant but a product of geopolymerization (Provis and Bernal 2014), they argued that water is not necessary for self-healing of geopolymer. Although the reason of the contradiction is unclear, the presence of metakaoline in the mixture might have resulted in long-term pozzolanic reactions that contributed to the self-healing. Further studies are needed to verify the hypothesis.

3.2. Stiffness recovery

In a previous study on self-healing ECC (Herbert and Li 2013), stiffness recovery was evaluated based on the chord modulus for stress levels between 0.5 and 2.0 MPa. However, it was found that the chord modulus between 0.5 and 2.0 MPa cannot fully reflect the stiffness profile of EGC in reloading. Figure 3 shows portions of typical stress-strain curves of W–1%, A–1%, and N–1% series during preloading and reloading, and corresponding chord modulus between 0.5 and 2.0 MPa for reloading. Nonlinearity can be seen in the reloading curve of a W–1% specimen compared to the corresponding chord. In contrast, deviation of the stress-strain curve from the chord is limited in both A–1% and N–1% specimens. The same trends were found in other specimens of all series. It is clear that the W–1% series had significantly higher residual stiffness in lower stress levels than those of the other series. Thus, in this study, stiffness recovery was evaluated based on chord modulus between 0.5 and 1.0 MPa.

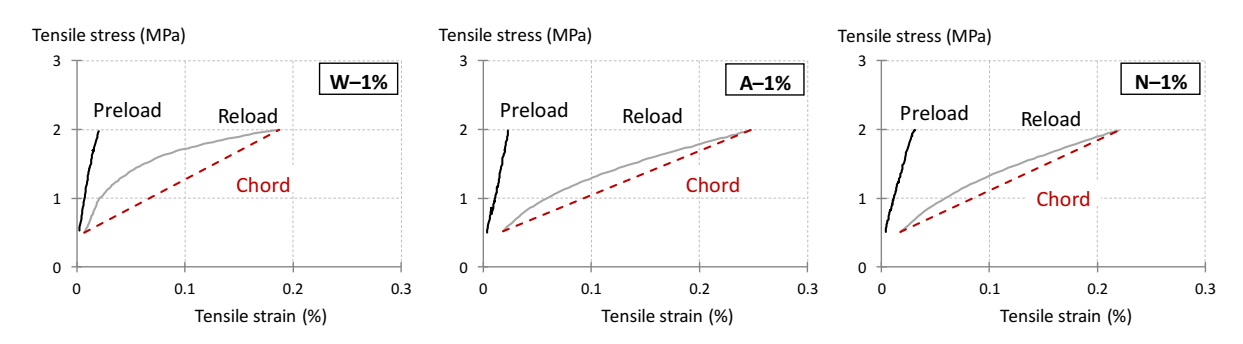


Figure 3. Plots of typical preloading and reloading stress-strain curves of each series for the stress range of 0.5 and 2 MPa, and corresponding chord modulus in reloading.

Table 3 lists the mean and standard deviations of initial and residual stiffness and the stiffness ratio for each series. The initial stiffness of W-1%, A-1%, and N-1% represents the chord modulus at the specimen age of 28 days measured in the preloading, while that of W-0% was measured after 120-day water curing. Relatively large variations in the initial stiffness can be seen in all series; coefficients of variation of W-1%, A-1%, N-1%, and W-0% are 11%, 26%, 21%, and 32%, respectively. Since EGC contains a small fiber volume of 2%, the initial elastic stiffness is mainly governed by matrix properties. Thus, these variations for the initial stiffness are likely related to material variability of the EGC matrix.

Table 3. Initial and residual	l stiffness and stiffness ratio	for the stress range of $0.5 - 1.0$ MPa.

Series	Initial stiffness $E_{0.5-1.0}$ (GPa)	Residual stiffness E'0.5-1.0 (GPa)	Stiffness ratio $R_{0.5-1.0}$ (%)
W-1%	10.4 ± 1.1	2.60 ± 0.91	24.6 ± 8.6
A-1%	8.1 ± 2.1	1.18 ± 0.17	15.5 ± 5.2
N-1%	7.0 ± 1.5	1.12 ± 0.09	16.2 ± 2.6
W-0%	6.9 ± 2.2	_	_

Despite the large variations, the results indicate the significantly higher residual stiffness and stiffness ratio of W-1% than those of A-1% and N-1%. Also, the residual stiffness and stiffness ratio of A-1% are similar to those of N-1%, which implies no performance recovery in the air-cured series. This agrees with the fact that microcracks were sealed in W-1% while no white precipitate was observed in A-1%. It should be also noted that no stiffness increase due to the water curing and 120-day aging has been confirmed; the initial stiffness of W-1% is rather larger than that of W-0%. Therefore, the higher residual stiffness of W-1% could be attributed to performance recovery due to the self-healing.

Compared to EGC used in this study, higher stiffness recovery has been reported for ECC materials. For example, Herbert and Li (2011) investigated self-healing of ECC under a natural environment. In their work, tensile strain of 1% was applied in preloading, and chord modulus between 0.5 and 2 MPa was used to evaluate the stiffness recovery. The mean stiffness ratios for specimens reloaded after 3-and 6-month natural environment exposures were 36% and 97% (i.e. almost full recovery), respectively. For a longer exposure of 12 months, the mean stiffness ratio reached 150%, meaning that the residual stiffness surpassed the initial stiffness. Herbert and Li (2011) pointed out that aside from self-healing, continued hydration of the cement matrix contributed to the high stiffness recovery.

There are several possible reasons for the limited stiffness recovery in EGC. Clearly, the limited formation of healing products is the most significant cause. Another possibility is that healing products in EGC have lower tensile strength that those in ECC, and a crack initiates in EGC healing products at a lower stress. This agrees with the fact that significant stiffness recovery was observed at lower stress levels in EGC. It is also possible that a crack initiates from the interface between the EGC matrix and healing products. This is the case if the bond between EGC matrix and healing products is weaker than that in ECC self-healing. Further research is needed to study cracking mechanisms in self-healed EGC.

While stiffness recovery in the present version of EGC is limited and only significant for low stress levels, the test results confirm the self-healing functionality of EGC with mechanical-performance recovery. Also, if most of microcracks could be completely healed, performance recovery could be significantly enhanced. To improve the self-healing functionality of EGC, a thorough understanding of healing mechanisms is important. The following SEM observation and EDS analysis of healing products provide some implications on the mechanisms.

3.3. SEM observation and EDS analysis

Figure 4 shows SEM micrographs of a healed microcrack in SEM-1% series. Most of the precipitates sealing the microcrack seem to have angular, stone-like shape as shown in Figure 4(a). Kan et al. (2010) reported that stone-like particles were formed within microcracks of self-healing ECC, and found to be mainly composed of calcite (CaCO₃). They also found fiber-like healing products, which were identified as C-S-H gels, but such substance was not observed in EGC. Instead, the magnified view of the healing products shown in Figure 4 (b) reveals the presence of spherical particles, which are likely to be unreacted fly ash. The presence of unreacted fly ash suggests a possibility of further geopolymerization (reaction between the unreacted fly ash and alkaline solution that may be supplied from some source) and/or pozzolanic reaction, which forms additional hardened matrix that can seal the crack.

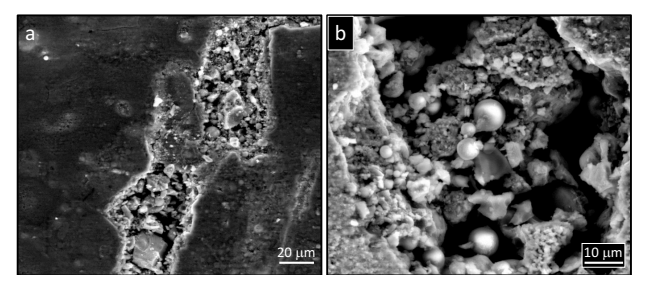


Figure 4. (a) SEM image of a microcrack and healing products sealing the crack and (b) magnified view of the healing products showing spherical unreacted fly ash.

Figure 5 shows the atomic percent of Na, O, C, Ca, Si, and Al along the scanned line. The sum of x-ray counts for these elements accounted for about 90% of the total detected counts. Concentrations of Si and Al show significant increases in the cracked region. The amount of Na does not significantly vary along the line, keeping the low level. A similar trend is found for C, except in a small region that has a

short peak. This peak might be associated with the presence of PVA fibers, which may be embedded near the surface and affect the analysis through the interaction volume of the electron beam.

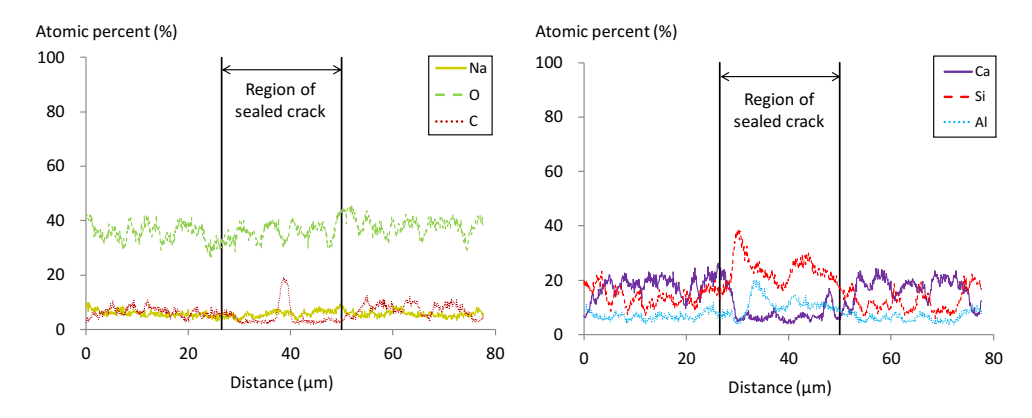


Figure 5. Elemental compositions detected along the scanned line.

The relatively low concentration of Na suggests that healing products are not salt deposits produced by reactions of cations leached from the pore solution with CO₂ in air (Provis and Bernal 2014). In a previous study by Zhang et al. (2013), efflorescence products in a fly ash-based geopolymer have been identified as Na₂CO₃·7H₂O. Geopolymer binders are mainly composed of aluminosilicate phases with a small amount of charge-balancing Na⁺ ions. Thus, if the healing products result from efflorescence, the relative concentration of Na should be higher in the region, which was not the case in the present result. EDS analysis also suggests that the healing products are not calcite (CaCO₃) in EGC as the region of the sealed crack shows a lower concentration of Ca compared to that of the geopolymer binder phase.

The x-ray mapping shown in Figure 6, which overlays information on the element concentration on top of the SEM image shown in Figure 1, confirms that the trend discussed above are consistent over the entire region of the microcrack. Higher concentrations are shown in higher brightness in the images. As can be seen, higher concentrations of Si and Al, and lower concentration of Ca are not limited to the area captured by line analysis but are visually evident over the entire cracked region.

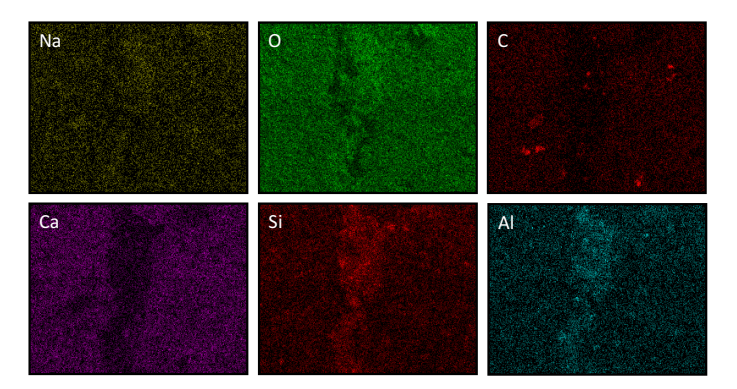


Figure 6. Elemental concentrations overlaid on top of the SEM image in Figure 1. Regions of higher concentration are shown in higher brightness.

The high concentration of Al and Si suggests that main products of EGC self-healing are some aluminosilicate compounds, which agrees with the study by Kan et al.(2019). Thus, the healing mechanism in EGC is different from both the calcite-dominated self-healing in cement-based materials or efflorescence in other fly-ash based geopolymers.

4. Conclusions

The self-healing functionality of EGC has been confirmed in the present study. In cracked EGC specimens subjected to water curing, white precipitates are formed, sealing the microcracks. This provides significant stiffness recovery in uniaxial tension for low stress levels of 0.5 - 1.0 MPa.

However, formation of healing products and the resultant mechanical performance recovery are limited in EGC compared to ECC materials. Additional geopolymerization or pozzolanic reaction through a supply of alkaline solution to the unreacted fly-ash in between microcracks provides a possible source of inducing further self-healing and improving mechanical performance recovery.

EGC healing products are mostly angular, stone-like substance, which is relatively rich in Si and Al, and has lower concentration of Ca, compared to the geopolymer matrix phase. This suggests that the main product of EGC self-healing is unlikely to be either calcite (CaCO₃) or salt deposits from efflorescence (Na₂CO₃), but rather a formation of some aluminosilicate compounds. Further study is required to fully understand the chemical nature of the healing products and corresponding reaction mechanisms. With that information, it would be possible to develop an effective method to improve the self-healing functionality of EGC.

Acknowledgements

The support from the National Science Foundation (Grant CMMI 1068005 and 1634694 to the University of Michigan) is gratefully acknowledged. The authors also acknowledge the material suppliers Headwaters Resources, PQ Corporation and Kuraray for providing materials used in this study.

References

- Ahn, T.H. and Kishi, T. (2010). Crack Self-healing Behavior of Cementitious Composites Incorporating Various Mineral Admixtures. Advanced Concrete Technology, 8(2), 171-186.
- Ali, M.K., Abu-Tair, A.I., Kinuthia, J.M., and Babecki, R. (2015). Self-healing and strength development of geopolymer concrete made with Waste by products. International Conference on Biological, Civil and Environmental Engineering, February, Bali, Indonesia.
- Duxson, P., Fernández-Jiménez, A., Provis, J.L., Lukey, G.C., Palomo, A., and Van Deventer, J.S.V. (2007). Geopolymer technology: The current state of the art. Materials Science, 42, 2917-2933.
- Herbert, E.N. and Li, V.C. (2013). Self-healing of microcracks in engineered cementitious composites (ECC) under a natural environment. Materials (Basel), 6(7) 2831–2845.
- Huang, H. and Ye, G. (2011). Application of sodium silicate solution as self-healing agent in cementitious materials. International RILEM Conference on Advances in Construction Materials Through Science and Engineering, September, Hong Kong, China.
- Jonkers, H.M., Thijssen, A., Muyzer, G., Copuroglu, O., and Schlangen, E. (2010). Application of bacteria as self-healing agent for the development of sustainable concrete. Ecological Engineering, 36(2), 230–235.
- Kan, L.L., Shi, H.S., Sakulich, A.R., and Li, V.C. (2010). Self-Healing Characterization of Engineered Cementitious Composite Materials. ACI Materials Journal, 107(6), 617–624.
- Kan, L.L., Lv, J.W., Duan, B.B., and Wu, M. (2019). Self-healing of Engineered Geopolymer Composites prepared by fly ash and metakaokin. Cement and Concrete Research, 125, 105895.
- Li, M. and Li, V.C. (2011). Cracking and healing of engineered cementitious composites under chloride environment. ACI Materials Journal, 108, 333–340.
- Liu, X., Ramos, M.J., Nair, S.D., Lee, H., Espinoza, D.N., and van Oort, E. (2017). True Self-Healing Geopolymer Cements for Improved Zonal Isolation and Well Abandonment. SPE/IADC Drilling Conference and Exhibition, March, The Hague, The Netherlands.
- Nishiwaki, T., Mihashi, H., Jang, B.K., and Miura, K. (2006). Development of Self-Healing System for Concrete with Selective Heating around Crack. Advanced Concrete Technology, 4, 267–275.
- Ohno, M. and Li, V.C. (2014). A feasibility study of strain hardening fiber reinforced fly ash-based geopolymer composites. Construction and Building Materials, 57, 163–168.
- Ohno, M. and Li, V.C. (2018). An integrated design method of Engineered Geopolymer Composite. Cement and Concrete Composites, 88, 73–85.
- Provis, J.L. and Bernal, S.A. (2014). Geopolymers and Related Alkali-Activated Materials, Annual Reviews of Materials Research, 44, 299–327.
- Qian, S.Z., Zhou, J., and Schlangen, E. (2010). Influence of curing condition and precracking time on the self-healing behavior of Engineered Cementitious Composites. Cement and Concrete Composites, 32, 686–693.
- Suryanto, B., Wilson, S.A., McCarter, W.J., and Chrisp, T.M. (2015). Self-healing performance of engineered cementitious composites under natural environmental exposure. Advances in Cement Research, 28, 211–220.
- Yang, Y., Yang, E., and Li, V.C. (2011). Autogenous healing of engineered cementitious composites at early age. Cement and Concrete Research, 41, 176–183.
- Zhang, Z., Wang, H., Provis, J.L., and Reid, A. (2013). Efflorescence: A Critical Challenge for Geopolymer Applications? Concrete Institute of Australia's Biennial National Conference, October, Gold Coast, Australia.